CHAPTER 24

A PARABOLIC REFRACTION-DIFFRACTION EQUATION

IN THE RAY-FRONT COORDINATE SYSTEM

Masahiko Isobe*

ABSTRACT

The parabolic equation method has been extensively used for combined refraction and diffraction problems of water waves. However, a parabolic equation is valid only when the direction of wave propagation nearly coincides with that of a coordinate; therefore, the validity ranges of the parabolic equations developed so far are restricted.

In order to achieve a wide range of validity, a parabolic equation is derived in this paper by employing a curvilinear coordinate system which has a pattern similar to that of wave rays and fronts. A computer program which is applicable to an arbitrary arrangement of coastal structures is then developed.

Results of numerical calculations are compared with available analytical solutions and laboratory data. It is proved that the present parabolic equation has a high accuracy for a wide range of incident wave direction and structure arrangement.

1. INTRODUCTION

In order to analyze the wave transformation due to combined refraction and diffraction, the mild-slope equation was derived by Berkhoff (1972). The mild-slope equation is an elliptic-type partial differential equation; hence the numerical calculation needs much computing time. Therefore, Radder (1979) and Tsay and Liu (1982) derived parabolic approximation equations which save a great amount of computing time and storage. Recently, the parabolic equation method has been modified in order to include the effects of wave nonlinearity (Kirby and Dalrymple, 1983; Liu and Tsay, 1984) and energy dissipation (Dalrymple et al., 1984; Liu and Tsay, 1985). However, the validity ranges of the parabolic equations are restricted due to the assumption that the direction of a coordinate nearly coincides with that of wave propagation.

The primary objective of this study is to derive a parabolic equation which is applicable even if the incident wave angle relative to the onshore direction and the longitudinal direction of a structure

^{*} Associate Professor, Department of Civil Engineering, Yokohama National University, 156 Tokiwadai, Hodogaya-ku, Yokohama, 240 Japan

PARABOLIC EQUATION

is large. This is done by employing a curvilinear coordinate system which has a pattern similar to that of wave rays and fronts. A computer program which can be applied to an arbitrary bottom profile and structure arrangement is developed. Results of numerical calculations are compared with available analytic solutions and laboratory data.

2. DERIVATION OF PARABOLIC EQUATION

2.1 Basic Concept

When Radder (1979) first derived a parabolic equation, Cartesian coordinates were employed. Therefore, if the incident wave angle is large, the direction of the coordinate significantly differs from that of wave propagation. In Tsay and Liu (1982), curvilinear coordinates following Snell's law were employed, which implies that the change in wave propagation direction due to refraction is taken into account. However, since the coordinates are determined independently of structures, a significant difference between the directions of the wave propagation and the coordinate occurs in the shadow region.

Waves are observed to propagate following Huygens' principle. If we define a coordinate system following this principle, the resulting coordinates must coincide with the wave ray and front pattern. We call this coordinate system a "ray-front coordinate system." Figure 1 shows an example of ray-front coordinate system. Rays 7 to 11 are incident wave rays, refracted by the change of water depth. Rays 1 to 5, and 12 and 13 are radiated from the tips of breakwaters and then refracted.

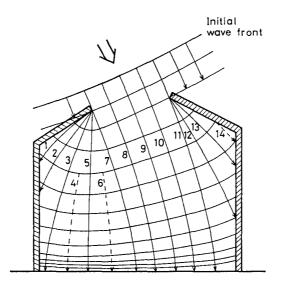


Fig. 1 Example of ray-front coordinate system.

Thus we can define a ray coordinate, and then a front coordinate from the orthogonality condition. By this definition, the direction of wave propagation almost coincides with that of the ray coordinate; therefore, the parabolic equation in this coordinate system is expected to be valid for a wide range of incident wave condition and structure arrangement.

2.2 Ray-front Coordinates

Consider curvilinear coordinates (ξ, η) as shown in Fig. 2. The directions of ξ and η respectively represent those of wave rays and fronts following Huygens' principle; thus the direction, α , of the ξ -coordinate can be determined by the following ray equation in the refraction problem:

$$\frac{1}{h_{\xi}}\frac{\partial\alpha}{\partial\xi} = \frac{1}{K}\frac{1}{h_{\eta}}\frac{\partial K}{\partial\eta}$$
(1)

where h_{ℓ} and h_{η} are the scale factors of the curvilinear coordinates; hence $h_{\ell}d\xi$ and $h_{\eta}d_{\eta}$ represent the lengths of short line elements. The quantity K is the wave number and usually can be calculated from the given local water depth by the dispersion relation. However, wave rays often intersects with each other for complicated bottom topographies; thus K is calculated from a slightly-modified water depth. The modified bottom topography may be taken as that with straight and parallel bottom contours, since a slight difference between the directions of the coordinate and wave propagation is allowed in the derivation of a parabolic equation. By this modification, the intersection of wave rays does not occur. The scales of axes are arbitrary; hence, we can take $h_{\ell} = h_{\eta} = 1/K$ without loss of generality, with which the values of the coordinates have the dimension of phase angle.

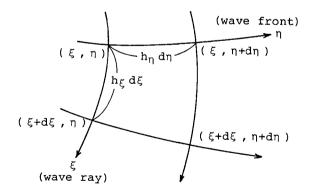


Fig. 2 Curvilinear coordinates

Once α is determined by Eq. (1), the position (x, y) along the ξ -coordinate can be calculated by

$$\frac{1}{h_{\xi}} \frac{d}{d\xi} (x, y) = (\cos \alpha, \sin \alpha)$$
⁽²⁾

If the position of a point on a front line is given, the position of the point advanced along a ray to the next shoreward front line can be determined by numerically integrating Eqs. (1) and (2) by the Runge-Kutta-Gill method. Then the η -axis can be determined as the line of ξ = const.

2.3 Parabolic Approximation

Berkhoff (1972) derived the mild-slope equation which governs the combined refraction and diffraction of periodic small-amplitude surface gravity waves over a seabed of a mild slope:

$$\overline{\nu}(G\overline{\nu}\phi) + k^2 G\phi = 0 \tag{3}$$

where $G = cc_g$ (c: wave celerity, c_g : group velocity), k is the wave number calculated from the given local water depth by dispersion relation, and V is the differential operator in the horizontal directions. The quantity ϕ represents the complex amplitude of the water surface fluctuation. From ϕ , the water surface fluctuation, ζ , and the velocity potential, ϕ , are expressed as

$$\zeta = \phi e^{-i\omega t} \tag{4}$$

$$\Phi = \frac{g}{i\omega} \frac{\cosh k(d+z)}{\cosh kd} \phi e^{-i\omega t}$$
⁽⁵⁾

where ω is the angular frequency, g the gravitational acceleration, d the given local water depth, z the vertical coordinate measured upward from the still water level, and t the time.

Equation (3) can be reexpressed in the curvilinear coordinates (ξ , η) as

$$\frac{1}{h_{\xi}h_{\eta}}\left\{\frac{\partial}{\partial\xi}\left(G\frac{h_{\eta}}{h_{\xi}}\frac{\partial\phi}{\partial\xi}\right) + \frac{\partial}{\partial\eta}\left(G\frac{h_{\xi}}{h_{\eta}}\frac{\partial\phi}{\partial\eta}\right)\right\} + k^{2}G\phi = 0$$
(6)

which is an elliptic-type partial differential equation. In the following, we approximate the mild-slope equation (6) to a parabolic equation following Radder (1979).

Equation (6) can be rewritten as

$$\frac{1}{h_{\xi}}\frac{\partial}{\partial\xi}\left(\frac{1}{h_{\xi}}\frac{\partial\phi}{\partial\xi}\right) = -\frac{1}{Gh_{\eta}}\frac{1}{h_{\xi}}\frac{\partial(Gh_{\eta})}{\partial\xi}\frac{1}{h_{\xi}}\frac{\partial\phi}{\partial\xi} - \left\{\frac{1}{Gh_{\xi}}\frac{1}{h_{\eta}}\frac{\partial}{\partial\eta}\left(G\frac{h_{\xi}}{h_{\eta}}\frac{\partial}{\partial\eta}\right) + k^{2}\right\}\phi \quad (7)$$

Here, we assume that ϕ can be splitted into two parts: the complex amplitudes ϕ^+ and ϕ^- due to incident and reflected waves, respectively, i.e.,

$$\phi = \phi^+ + \phi^- \tag{8}$$

$$\phi^{\pm} \sim a^{\pm} \exp\left(\pm i \sqrt{kh_{\xi} d\xi}\right) \tag{9}$$

From Eqs. (8) and (9), we have

$$\frac{1}{h_{\xi}}\frac{\partial\phi}{\partial\xi} = ik\phi^{+} - ik\phi^{-} \tag{10}$$

Then, we can eliminate ϕ^- from Eqs. (8) and (10):

$$\phi^{+} = \frac{1}{2}\phi + \frac{1}{2ik}\frac{1}{h_{\xi}}\frac{\partial\phi}{\partial\xi}$$
(11)

By taking the gradient of Eq. (11) in the direction of ξ and substituting Eq. (7), we obtain

$$\frac{1}{h_{\xi}} \frac{\partial \phi^{+}}{\partial \xi} = -\frac{1}{2ik} \left\{ \frac{1}{Gh_{\xi}} \frac{1}{h_{\eta}} \frac{\partial}{\partial \eta} \left(G \frac{h_{\xi}}{h_{\eta}} \frac{\partial}{\partial \eta} \right) + k^{2} \right\} \phi \\ + \left\{ \frac{1}{2} - \frac{1}{2ik^{2}} \frac{1}{h_{\xi}} \frac{\partial k}{\partial \xi} - \frac{1}{2ik} \frac{1}{Gh_{\eta}} \frac{1}{h_{\xi}} \frac{\partial (Gh_{\eta})}{\partial \xi} \right\} \frac{1}{h_{\xi}} \frac{\partial \phi}{\partial \xi}$$
(12)

On substituting Eqs. (8) and (10), we have a differential equation which contains ϕ^+ and ϕ^- . Here, we further assume that $|\phi^+| >> |\phi^-|$, i.e., $\phi^+ = \phi$ and $\phi^- = 0$. Thus we finally obtain the following parabolic equation for ϕ :

$$\frac{1}{Gh_{\xi}}\frac{1}{h_{\eta}}\frac{\partial}{\partial\eta}\left(G\frac{h_{\xi}}{h_{\eta}}\frac{\partial\phi}{\partial\eta}\right)+2ik\frac{1}{h_{\xi}}\frac{\partial\phi}{\partial\xi}+\left\{\frac{i}{Gh_{\eta}}\frac{1}{h_{\xi}}\frac{\partial}{\partial\xi}(kGh_{\eta})+2k^{2}\right]\phi=0$$
(13)

In order to make the change of ϕ slower, we transform the unknown variable from ϕ to ψ as

$$\phi = \psi \exp\left(i \int K h_{\xi} d\xi\right) \tag{14}$$

Since K is the approximate local wave number, the exponential term in the above equation roughly represents the phase of ϕ ; hence, the spatial change of ϕ is expected to become slow. On substituting Eq. (14) into Eq. (13), we obtain the following parabolic equation for ϕ :

$$\frac{1}{Gh_{\varepsilon}}\frac{1}{h_{\eta}}\frac{\partial}{\partial\eta}\left(G\frac{h_{\varepsilon}}{h_{\eta}}\frac{\partial\phi}{\partial\eta}\right)+2ik\frac{1}{h_{\varepsilon}}\frac{\partial\phi}{\partial\xi}+\left\{\frac{i}{Gh_{\eta}}\frac{1}{h_{\varepsilon}}\frac{\partial}{\partial\xi}(kGh_{\eta})+2k(k-K)\right]\phi=0 \quad (15)$$

Equation (15) is parabolic; therefore, we can numerically solve it step by step from offshore to onshore if adequate boundary conditions are given. It should be noted that Eqs. (13) and (15) agree with those of Radder (1979) when they are described in Cartesian coordinates.

In deriving parabolic equations, we can adopt slightly different assumptions, obtaining different equations in high-order terms. However, the result of numerical calculation showed that the present parabolic equation has the highest accuracy among several possible equations.

2.4 Physical Interpretation of Parabolic Equation

Following Berkhoff et al. (1982), we separate the amplitude and phase of ϕ as

$$\psi = a e^{i\epsilon} \tag{16}$$

On substituting Eq. (16) into Eq. (15), we have

$$\frac{1}{h_{\ell}} \frac{\partial \varepsilon}{\partial \xi} = k - K - \frac{1}{2k} \left(\frac{1}{h_{\eta}} \frac{\partial \varepsilon}{\partial \eta} \right)^2 + \frac{1}{2akGh_{\ell}} \frac{1}{h_{\eta}} \frac{\partial}{\partial \eta} \left(G \frac{h_{\ell}}{h_{\eta}} \frac{\partial a}{\partial \eta} \right)$$
(17)

$$\frac{1}{h_{\xi}h_{\eta}} \left[\frac{\partial}{\partial \xi} (a^2 k G h_{\eta}) + \frac{\partial}{\partial \eta} \left(a^2 \frac{1}{h_{\eta}} \frac{\partial \varepsilon}{\partial \eta} G h_{\xi} \right) \right] = 0$$
(18)

from real and imaginary parts, respectively. Equation (17) can be rewritten as

$$\left(K + \frac{1}{h_{\epsilon}} \frac{\partial \varepsilon}{\partial \xi}\right)^{2} + \left(\frac{1}{h_{\eta}} \frac{\partial \varepsilon}{\partial \eta}\right)^{2} = k^{2} + \left\{k - \left(K + \frac{1}{h_{\epsilon}} \frac{\partial \varepsilon}{\partial \xi}\right)\right\}^{2} + \frac{1}{aGh_{\epsilon}} \frac{1}{h_{\eta}} \frac{\partial}{\partial \eta} \left(G \frac{h_{\epsilon}}{h_{\eta}} \frac{\partial a}{\partial \eta}\right)$$
(19)

Equation (19) corresponds to the eikonal equation in refraction problems but includes the effect of diffraction in the η -direction as seen from the last term on the right hand side.

Since $G = \omega c_g/k$, Eq. (18) represents the conservation of wave energy. In the first parentheses, however, the ξ -component of the wave number should appear instead of k itself. Therefore, if the direction cosine in the ξ -direction is significantly less than unity, i.e., the direction of wave propagation is significantly different from the ξ direction, the error of the present parabolic equation will become large. Usually this does not occur, since the coordinates are determined following Huygens' principle.

2.5 Boundary Condition

The condition of complete reflection is imposed on fixed boundaries; thus the derivative of ϕ in the normal direction of the boundaries becomes zero. This can be expressed in terms of ϕ as

$$\frac{1}{h_{\eta}}\frac{\partial\phi}{\partial\eta} - \left(\frac{1}{h_{\xi}}\frac{\partial\phi}{\partial\xi} + iK\phi\right)\tan\delta = 0$$
(20)

where δ denotes the direction angle of the boundary measured from the ξ -direction toward the η -direction.

The first term in the parentheses of Eq. (20) is usually small compared to the second term; therefore, it can be neglected as

$$\frac{1}{h_{\eta}}\frac{\partial\phi}{\partial\eta} - iK\phi\tan\delta = 0$$
(21)

The accuracy of numerical caculation was higher when Eq. (21) was adopted as the boundary condition than when Eq. (20) was adopted. The reason of this result is not clear, but the error of Eqs. (18) and (21)

may cancel with each other. Hereafter, Eq. (21) will be used for boundary conditions.

For open boundaries, Eq. (21) with $\delta = 0$ was used. This means that the waves propagate in the ξ -direction just by refraction and the gradient in the η -direction is zero. If the open boundaries are located far from structures, they give no influence on the wave field around structures. However, once the disturbance from structures reaches the open boundary, the present condition induces the reflection of the disturbance.

3. PROCEDURE OF NUMERICAL CALCULATION

In order to determine the ray-front coordinates, Eqs. (1) and (2) were integrated by the Runge-Kutta-Gill method. The Crank-Nicholson scheme in which the weights for the old and new front lines are equal was applied to solve the parabolic equation (15). The weights for the two lines in the boundary condition were also taken equal.

The procedure of numerical calculation is summarized as follows:

- 1) Determine the position of an initial front line and the values of ϕ on the line from Snell's law.
- 2) Determine the position of the front line at the next step by Eqs. (1) and (2). From the tip of a structure, new wave rays are added as rays 1,2,3 and 5, or 12 and 13 in Fig. 1. If the distance between two adjacent rays exceeds a given value, new rays are also added by interpolation as rays 4,6, and 14 in Fig. 1.
- 3) Solve the parabolic equation (15) in order to determine the value of ϕ on the new front line.
- 4) Repeat 2) and 3) until the domain of calculation is covered with the ray-front coordinates.

A FORTRAN program which can be applied to an arbitrary incident wave condition, boundary condition, and bottom topography was developed.

4. RESULTS

4.1 Comparison with Analytical Solutions

In Fig. 3, circles show calculated wave height changes due to refraction. Waves are incident obliquely to a plane sloping beach with a slope of 1/10. In the figure, θ_0 denotes the wave angle in deep water, d/L_0 the ratio of local water depth to deep-water wavelength, and H/H_0 the ratio of local wave height to deep-water wave height. In the numerical calculation shown in this figure, the grid size to wavelength ratio, d/L, is 1/20, which was proved to be sufficiently small by numerical experiment. Solid lines indicate wave height

changes obtained by Snell's law. The agreement is good even if the incident wave angle is large.

Next, the diffraction coefficient due to semi-infinite breakwater is examined. Figure 4 shows the diffraction coefficient along the line from A to B and from B to C. Various symbols indicate the results of the present numerical calculations with various grid sizes. The analytical solution by Penny and Price (1952) is shown by a curve. Though the small oscillation from A to B is not accurately reproduced, the agreement is good on the whole. Figure 5 compares the numerical and analytical diffraction coefficients behind a semi-infinite breakwater for various incident wave directions. The agreement is good for a wide range of incident wave direction.

Figure 6 compares the wave height distribution in front of the breakwater. Since the ray-front coordinates are defined from the direction of the incident waves, the ξ -direction can be significantly different from the propagation direction of the reflected waves. Therefore, as seen from the open triangles in Fig. 6(b), the calculated oscillation of wave height differs significantly from the analytical solution. A mirror image technique was employed to improve the accuracy of calculation in the reflective region: 1) the semi-infinite breakwater is first removed, 2) a numerical solution is obtained for a semi-infinite breakwater with θ_0 =-90° (this value does not change the result significantly), and 3) the solution is folded along the given semi-infinite breakwater and superimposed. Closed symbols indicate the results; the agreement between the numerical and analytical results become much better.

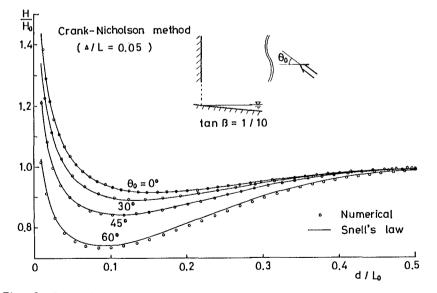


Fig. 3 Comparison of numerical and analytical wave height changes due to refraction.

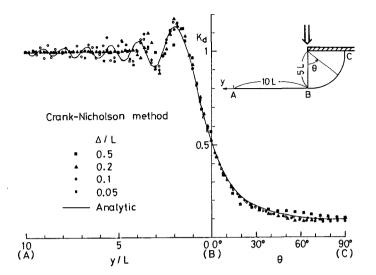


Fig. 4 Effect of grid size on the diffraction coefficient around a semi-infinite breakwater.

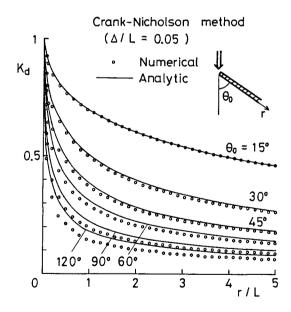


Fig. 5 Comparison of numerical and analytical diffraction coefficients just behind a semi-infinite breakwater.

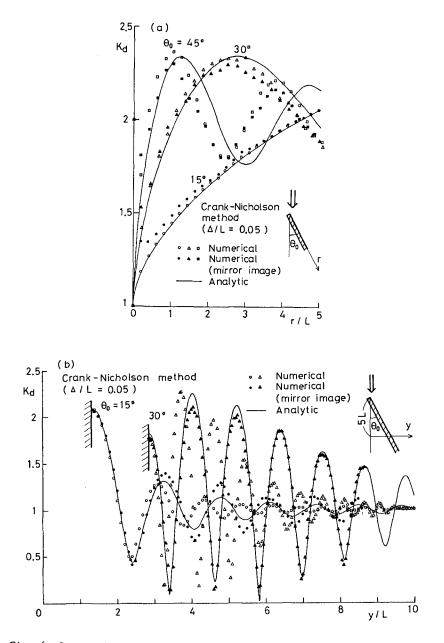


Fig. 6 Comparison of numerical and analytical wave height distributions in front of a semi-infinite breakwater.

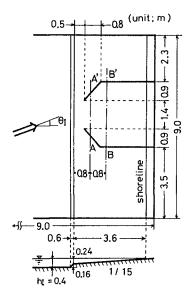
4.2 Comparison with Experimental Data

Figure 7 shows the present experimental apparatus. A wave basin which is 9m wide and 9m long was used. As seen in the figure, a plane beach with a slope of 1/15 was attached and breakwaters were arranged on the beach. A flap-type wave maker was set obliquely to the wave basin. Capacitance wave gages were used to measure the water surface fluctuation. The incident wave height, period, and angle were 9.1cm, 0.83s, and 18°, respectively.

Figure 8 compares the calculated and measured wave height distributions from A to A' and from B to B'. The agreement is fairly good. In shallower region, time history of water surface fluctuation becomes asymmetrical due to nonlinear effect; hence comparison was not made.

5. CONCLUSION

Curvilinear coordinates which follow Huygens' principle and are named ray-front coordinates were introduced. In the coordinates, a parabolic equation for combined refraction and diffraction of water waves was derived. Numerical calculation was carried out and the results were compared with available analytical solutions and experimental data.



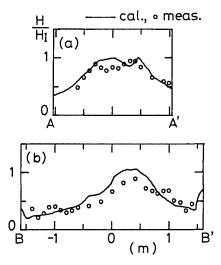


Fig.8 Comparison of calculated and measured wave height distributions.

Fig. 7 Experimental apparatus.

The present method was proved to have a high accuracy for refraction and diffraction of linear water waves. However, in the reflective region, direct application of the parabolic equation yields a significant error because incident and reflected waves exist in the region. The accuracy of the numerical calculation was improved by employing a mirror image technique.

REFERENCES

- 1) Berkhoff, J. C. W. (1972): Computation of combined refractiondiffraction, Proc. 13th Coastal Eng. Conf., ASCE, pp.471-490.
- Berkhoff, J. C. W., N. Booy and A. C. Radder (1982): Verification of numerical wave propagation models for simple harmonic linear water waves, Coastal Eng., Vol. 6, pp. 253-279.
- 3) Dalrymple, R. A., J. T. Kirby and P. A. Hwang (1984): Wave diffraction due to areas of energy dissipation, J. Waterway, Port, Coastal and Ocean Eng., ASCE, Vol. 110, pp. 67-79.
- 4) Kirby, J. T. and R. A. Dalrymple (1983): A parabolic equation for the combined refraction-diffraction of Stokes waves by mildly varying topography, J. Fluid Mech., Vol. 136, pp. 453-466.
- 5) Liu, P. L.-F. and T.-K. Tsay (1984): Refraction-diffraction model for weakly nonlinear water waves, J. Fluid Mech., Vol. 141, pp. 265-274.
- 6) Liu, P. L.-F. and T.-K. Tsay (1985): Numerical prediction of wave transformation, J. Waterway, Port, Coastal and Ocean Eng., ASCE, Vol. 111, pp. 843-855.
- 7) Penny, W. G. and A. T. Price (1952): The diffraction theory of sea waves and the shelter afforded by breakwaters, Phil. Trans. Roy. Soc. Lond., Ser. A, Vol. 244, pp. 236-253.
- 8) Radder, A. C. (1979): On the parabolic equation method for waterwave propagation, J. Fluid Mech., Vol. 72, pp. 373-384.
- 9) Tsay, T.-K. and P. L.-F. Liu (1982): Numerical solution of waterwave refraction and diffraction problems in the parabolic approximation, J. Geophys. Res., Vol. 87, pp. 7932-7940.